Freeform Object Positioning by 3D Shape Matching Without Artificial Feature Points

J.S.M. Vergeest
Delft University of Technology
Delft, The Netherlands
j.s.m.vergeest@io.tudelft.nl

Y. Song
Delft University of Technology
Delft, The Netherlands
y.song@io.tudelft.nl

D. Hartge
Delft University of Technology
Delft, The Netherlands
d.hartge@student.hhs.nl

ABSTRACT

Determining the position and orientation of a workpiece relative to a manufacturing device is a prerequisite for machining path planning. If the workpiece is freeform and if it contains no predefined feature points, then object positioning and tool calibration can be accomplished using shape matching in 3D space. In this paper we study the feasibility and accuracy of non-contact, featureless positioning based on matching of a CAD model to a 3D scan of the object once it is physically mounted. The invariance of the placement of the 3D scanner is verified and the spread in the transformation parameters is analyzed. The matching is performed using a least-squares and a Hausdorff shape difference measure. The effect of point cloud size on the accuracy is analyzed. Recommendations for improvement and applications are provided.

Keywords
3D shape matching, freeform objects, workpiece calibration, transformation accuracy

1. INTRODUCTION

Determining the accurate position and orientation of a mechanical part relative to a manufacturing device is commonly dependent on clearly distinguishable corners, edges or faces of the object. Those features are either measured or manually adjusted, thus implementing a calibration procedure. Robot teaching is based on such procedures, where for example an assembly or welding process is manually pre-played by an operator, and can be repeated accurately by the robot from then on. In other applications, where the machining path is computed offline, the workpiece should be placed or clamped in such a way that the toolpath coordinates are generated in a compatible way. A toolpath generator computes points relative to the workpiece. The coordinates of these points are ultimately sent to a manufacturing device. If the placement of the workpiece relative to the

manufacturing device differs from the placement asumed by the toolpath generator, a correction matrix to compensate for the difference should displace all points. Alternatively, if the placement of the workpiece is explicitly known beforehand, it can be assured that the toolpath generator delivers the correct coordinates.

There are many ways to measure the placement of a part relative to some reference frame. Mechanical probing devices can be used or non-contact instruments such as CCD cameras, laser pointers or 3D scanning systems. As mentioned, when the object contains "simple" recognizable features, the correspondence between measured data and places on the geometry can easily be established and hence the placement of the entire object can be derived (Pessel 2003), (González-Galván 2003).

In this paper we deal with a workpiece which is freeform and may contain no obvious features at all. The workpiece can, for example, be a manually produced clay model, resulting from a shape design exploration. At the very early stages of product design, traditional modeling methods such as sketching and claying are sometimes preferred over the use of any computer modeling or CAD system (Prieto 2003). However, at a certain stage of the design process, the physical model should be transferred to the computer for analysis, simulation

and manufacturing purposes. In principle one could use existing technologies of reverse engineering for this, including 3D digitization of the object, surface reconstruction from the measured points and finally the creation of a CAD model (Várádi 1997). However, we aim to support a more complicated application, consisting of the following steps:

1. Manual creation of a model out of material, for example clay. The designer realizes that the next shape modifications could be easier achieved using a CAD system rather than manually.

2. The model is 3D digitized and imported into a CAD/CAM system.

3. Using a machining planning module of the CAD system, the wanted modifications are made to the CAD model and a toolpath is generated.

4. The clay model of step 1 is placed in front of a machining device, and the shape modifications are effectuated on the physical model by device.

5. The clay model is removed from the device and the designer resumes the manual modeling process.

Theoretically, step 3 could be performed using a common rapid prototyping method. However, then the entire model should be reproduced by 3D printing or other additive technique, which would result in an object of a different, non-clay material. Another option would be to produce the entire object out of a rectangular stock of clay by milling. This, however, is very costly and time consuming. Instead, in step 3 only the modifications as intended in step 1 are computed, as a relatively small toolpath. In step 4, only this small toolpath is executed, directly on the clay model. Using this method, material is selectively removed. If the shape modification intended in step 1 implies the local addition of a shape feature, then a lump of clay can be roughly deposited immediately after step 1, and the feature can still be realized using the procedure described.

When, in step 4, the clay model is placed in front of the milling device, the exact position and orientation of the model should be known to assure that the toolpath calculated in step 3 is compatible with the actual setup.

A formal definition of the problem just described is given in section 2. In section 3 the method to obtain the required transformation is presented. The robustness and accuracy of the transformation is numerically analyzed in section 4 and some examples are provided. Conclusions are drawn in section 5.

2. PROBLEM STATEMENT
Notation
We adopt a common notation for points and vectors in R^3 as four-vectors with 4th component 1 and 0 respectively. A coordinate system or frame A is represented by a 4×4 matrix containing the x-, y- and z-directions of A as unit vectors in the 1st, 2nd and 3rd column and the 4th column contains the origin of A. If A is defined relative to another frame B then the matrix is denoted ^BA. A point p and vector v is denoted ^Bp and ^Bv if they are defined relative to frame B. If a point is represented by ^Ap relative to frame A and if the same point is represented by ^Bp relative to frame B, then $^Bp = {}^BA\,{}^Ap$ and hence ^BA serves as a rigid-body transformation matrix.

Problem
Given:

- A geometric representation ^BP defined relative to a base coordinate system B. ^BP represents a physical object P called platform, which serves as a global reference object.

- A geometric representation ^XA relative to an arbitrary frame X. ^XA represents a physical design part or a manually made object out of clay, for example. The shape of A can be freeform and does not contain predefined feature points. Frame X is arbitrary and could be the coordinate system of a 3D scanner with which the object was digitized or X could be a coordinate system of a CAD system in which the scanned object was imported.

- A set of points ^Xm defined relative to X. The set defines a process to be carried out on the physical part A. Normally, ^Xm defines a toolpath, for example for a milling device that should remove some material from the physical part A., where the toolpath is computed relative to X.

Wanted:

- The transformation W yielding the toolpath ^Bm, which can be executed onto to the physical part A once placed in the vicinity of P. Here $^Bm = W\,{}^Xm$ and hence $W = {}^BX$ is the transformation from X to B.

Approach
The approach to this problem is as follows. First the placements of P and of A each are determined relative to a scanning device frame S, yielding ^SP

and ^{S}A, respectively. Since P and A were already known relative to B and X, respectively, the relative placements ^{S}X and ^{S}B can be found by shape matching.. Finally the transformation W can be calculated as $W = (^{S}B)^{-1}\ ^{S}X = ^{B}S\ ^{S}X = ^{B}X$.

The method should work even if A contains no "obvious" features such as corners and edges. This restriction is not necessary for object P.

# 3. DESCRIPTION OF THE METHOD
Experimental set-up
As described in the introduction, the method is applied to (but not limited to) manually created objects (for example using clay), of almost arbitrary shape. The device that effectuates the modifications, defined using any machining package is a 6 degrees-of-freedom industrial robot of Siemens/Manutec, manipulating a milling device, see Fig. 1. The platform on which the workpiece is placed is rotating about a vertical axis, thus making the system a 7-DoF equipment called the Sculpturing Robot (Tangelder 1998). The accuracy of a milling process, after mechanical calibration of the robot, is between 0.3 and 0.6mm, depending on the region in workspace (Broek 1996).
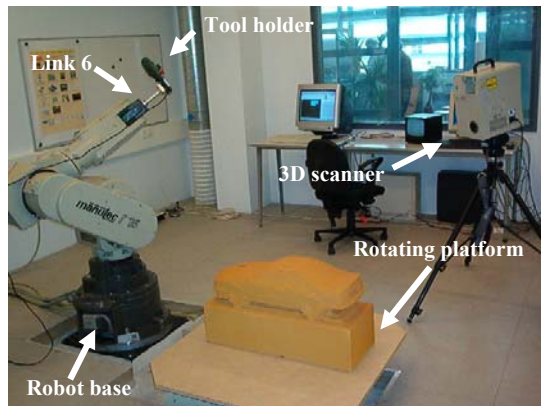
Figure 1. A 6-DoF robot manipulating a milling device performs selective clay milling. The device on the tripod is the 3D scanner

Object scanning is performed by a Minolta VI-700 3D Digitizer, capable of scanning 40,000 points in 0.6s. The scanning window can vary between 70×70mm and 1100×1100mm due to the zoom lens. The distance to the object is adjustable between 0.6 and 2.5m. At the shortest distance the xy-resolution is 0.35mm and the z-resolution is 0.11mm.

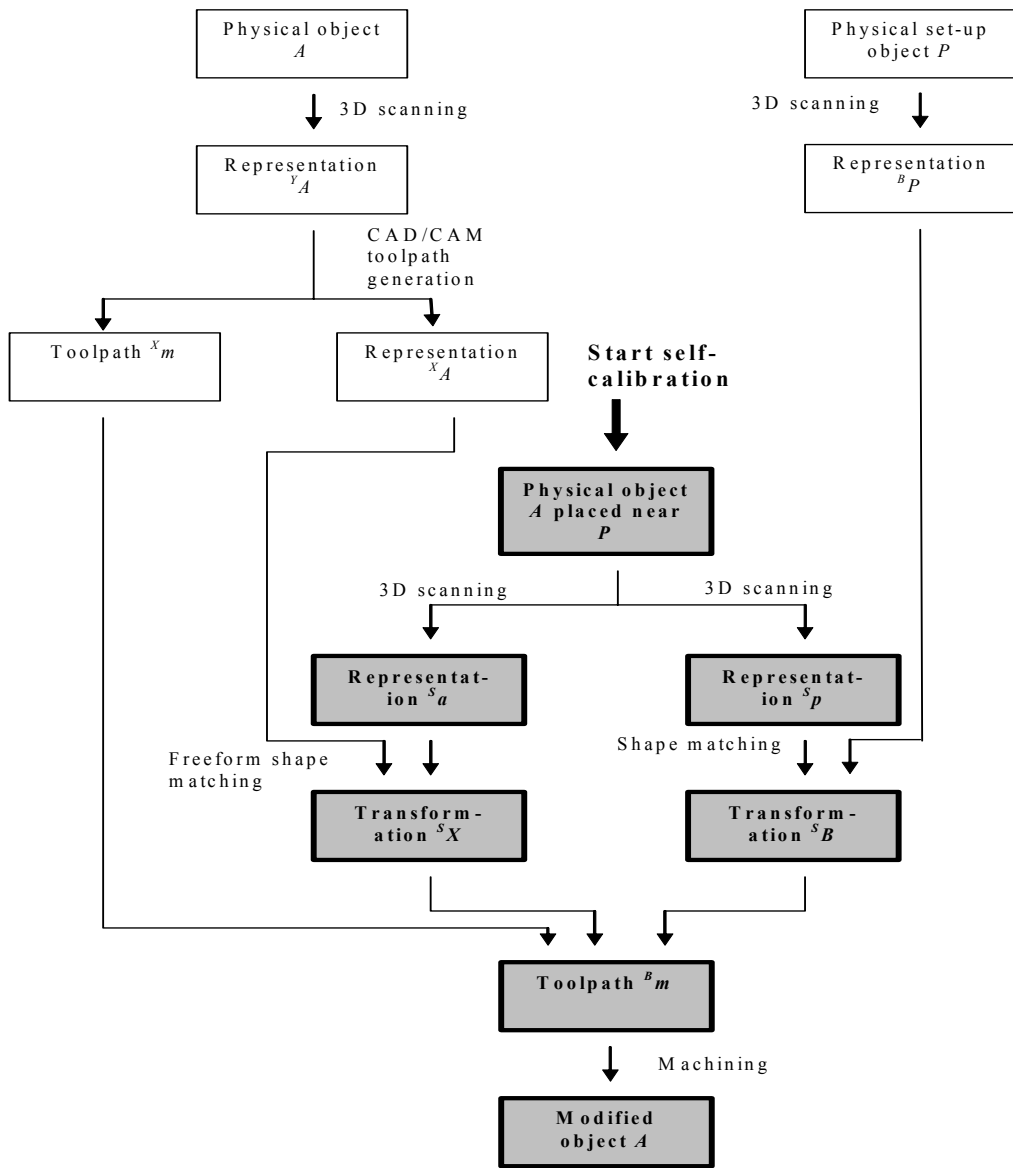The placements of the frames of robot, platform and scanner are depicted in Figure 2.
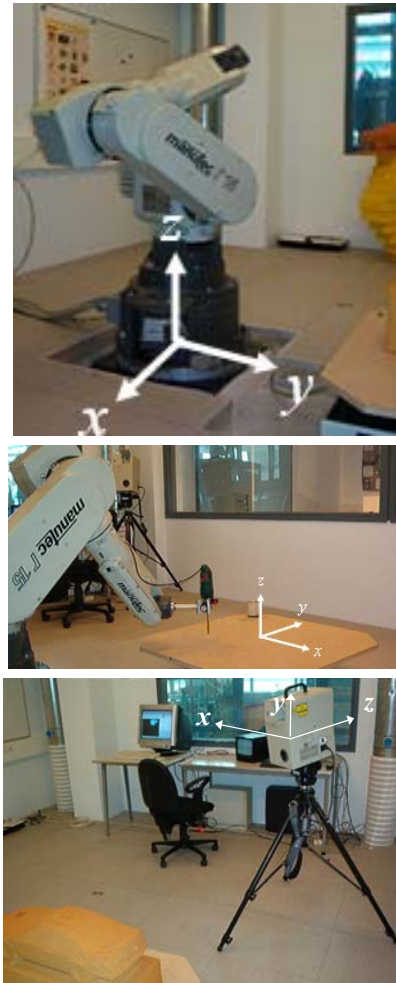
Figure 2. Top to bottom: Placements of the frames B, Q and S, respectively.

Figure 3. Workpieces have been placed on the platform, near the L-shaped reference object P. A top view is shown on the right. Both test objects A_1 and A_2 are shown, a small (2cm diameter) puppet and a 25cm car model, respectively.

```
┌─────────────────┐                          ┌─────────────────┐
│ Physical object │                          │ Physical set-up │
│       A         │                          │    object P     │
└─────────────────┘                          └─────────────────┘
        │ 3D scanning                    3D scanning │
        ▼                                            ▼
┌─────────────────┐                          ┌─────────────────┐
│ Representation  │                          │ Representation  │
│      ᵞA         │                          │      ᴮP         │
└─────────────────┘                          └─────────────────┘
```

Figure flow: Physical object A → (3D scanning) → Representation ^YA → (CAD/CAM toolpath generation) → Toolpath ^Xm and Representation ^XA

Physical set-up object P → (3D scanning) → Representation ^BP

Start self-calibration → Physical object A placed near P → (3D scanning) → Representation ^Sa and Representation ^Sp

Representation ^Sa → (Freeform shape matching) → Transformation ^SX

Representation ^Sp → (Shape matching) → Transformation ^SB

Transformation ^SX and Transformation ^SB and Toolpath ^Xm → Toolpath ^Bm → (Machining) → Modified object A

Figure 4. Procedure of the semi-automatic calibration process

In the current stage of research the platform is not revolving and therefore we consider Q as a fixed reference frame known relative to B. To ease the usage of the geometry of the platform as a reference shape P, an L-shaped object with rectangular faces is permanently put on top of the platform (Figure 3). The shape of this reference object contains clearly visible corners and edges as to ease shape matching later. However, the actual dimensions of P need not explicitly to be known.

Also note that, unlike object A, object P may contain artificial features.

Procedure

The calibration procedure is depicted in Fig. 4. From the users point of view the process begins at "start self-calibration", where the physical model is placed on the platform in front of the Sculpturing Robot. We recall that, according to the problem statement in Section 2, we have already available the representations ^XA and ^BP and a set of toolpath points ^Xm.

The 3D scanner digitizes the scene containing the physical objects A and P. Alternatively, two data captures can be made with different focal distances of the zoom lens, provided that the scanner device is not displaced between the shots. The data contain point clouds representing a portion ^Sa of the surface of A and a portion ^Sp of the surface of P. The point set ^Sa must be compatible with a portion of the point set ^XA, up to a coordinate transformation U, and the similar should hold for set ^Sp up to the transformation V.

There is no explicit correspondence between points in the sets ^Sa and ^XA. Therefore the transformation U should be estimated by matching the two sets, such that $D(^Sa,\ U\ ^XA)$ is minimized, where D is a shape dissimilarity measure (Veltkamp 2001). U can be interpreted as the transformation matrix ^SX, defining the placement of frame X relative to scanner S. The transformation can be parameterized with three rotations R by Euler angles φ_u , θ_u and ψ_u about local z-, y- and z-axes, followed by a translation T along a vector $(x_u, y_u, z_u)^T$,

$$U(x_u, y_u, z_u, \varphi_u , \theta_u, \psi_u)$$
$$= T(x_u, y_u, z_u)\ R_z(\varphi_u)\ R_y(\theta_u)\ R_z(\psi_u),$$

following the Euler Z-Y-Z convention (Latombe 1991). How the values of the 6 parameters that minimize $D(^Sa,\ U\ ^XA)$ are determined will be described later in this section.

Similarly, the point sets ^Sp and ^BP are matched by minimizing $D(^Sp,\ V\ ^BP)$, V can be interpreted as the transformation matrix ^SB defining the placement of frame B relative to S. Finally, the placement of frame X relative to the base frame B can be derived as:

$$W = {}^BX = {}^BS\ {}^SX = V^{-1}\ U. \qquad (1)$$

Using the matrix W the toolpath ^Xp generated relative to X can be transformed to the toolpath relative to the robot base:

$$^Bp = W\ ^Xp.$$

The transformation matrix W can also be regarded as rotation followed by a translation. If we define w as the 6-vector $w = (x_w, y_w, z_w, \varphi_w , \theta_w, \psi_w)^T \in \mathbb{R}^3 \times SO(3)$ then

$$W(w) = T(x_w, y_w, z_w)\ R_z(\varphi_w)\ R_y(\theta_w)\ R_z(\psi_w),$$

where the translation vector and Euler angles can be derived from the matrix $W = \{w_{ij}\ , i, j = 1, ...4\}$:

$x_w = w_{14},\ y_w = w_{24},\ z_w = w_{34},$

$\varphi_w = \text{atan2}(w_{23}, w_{13})$

$\theta_w = \text{atan2}(\text{sqrt}(w_{31}{}^2 + w_{32}{}^2), w_{33})$

$\psi_w = \text{atan2}(w_{32}, -w_{31}).$

The three subsequent rotations can be replaced by one single rotation by angle Ω about the so-called principle axis, where Ω is given by

$$\Omega = \text{acos}\left(\frac{w_{11} + w_{22} + w_{33} - 1}{2} \right)$$

(Craig 1989). If two matrices differ little in their principle axis rotation, then they can be interpreted as having nearly the same orientation.

Shape matching

To determine the matrices U or V, a match of two point clouds must be found, where each point cloud represents the surface of a shape, or a portion of that surface. In the particular application of this work, we need a method to minimize the distance between two point sets, called A and B here, where it can be assumed that only a partial match of A with B is required, i.e. A needs to be compatible with a portion of B only. A partial match of A to B is achieved for

$$u = \text{arg}(\min_u D(A, U(u)B),$$

where $u = (x_u, y_u, z_u, \varphi_u , \theta_u, \psi_u)^T$. The similar notation applies to V and v. There are several ways to solve the minimization problem (Bessl 1992). In this paper we consider only two methods. The first is based on a least-squares difference between point set A and point set B using

$$D(A, U(u)B) = \frac{1}{n_A} \sum_{i=1}^{n_a} | a_i - b_i |^2 ,$$

where n_a is the number of points in A, $a_i \in A$ and $b_i \in U(u)B$ is a point that is in some way related (corresponding) to point a_i. In case the sets A and B have the same number of points, which are pair-wise corresponding, then the definition of b_i is trivial. In the general case b_i is often defined as the point in $U(u)B$ closest to a_i, as, for example, in the Iterative Closest Point algorithm (Bessl 1992).

Commercial packages for scan data registration often take advantage of the known connectivity among points in a point set; typically they generate a triangular mesh bounding the set. The computation of the distance of a given point to a triangular mesh can be significantly faster than finding the point from an unordered set which is closest to the given point. An iteration step for $u \in \mathbb{R}^3 \times SO(3)$ (or alternatively, using quaternions) can be estimated from the set of difference vectors associated to the corresponding pairs of points. $SO(3)$ denotes the special group of orthonormal matrices in 3 dimensions.

Since in our application we should not assume that the scanned data is converted into a triangulation, we also considered the Mean Directed Hausdorff distance from the set A to the set $U(u)B$, defined as

$$H(A,U(u)B) = \frac{1}{n_A} \sum_{i=1}^{n_a} (\min_{j} |a_i - b_j|),$$

where a_i and b_j are points from A and $U(u)B$, respectively.

We have developed an accelerated version of the MDH to reduce the search among points in $U(u)B$. The reduction is based on a pre-computed three-dimensional space binning (Spanjaard 2001). The iteration for u is computed by sampling derivatives of H around the current transformation.
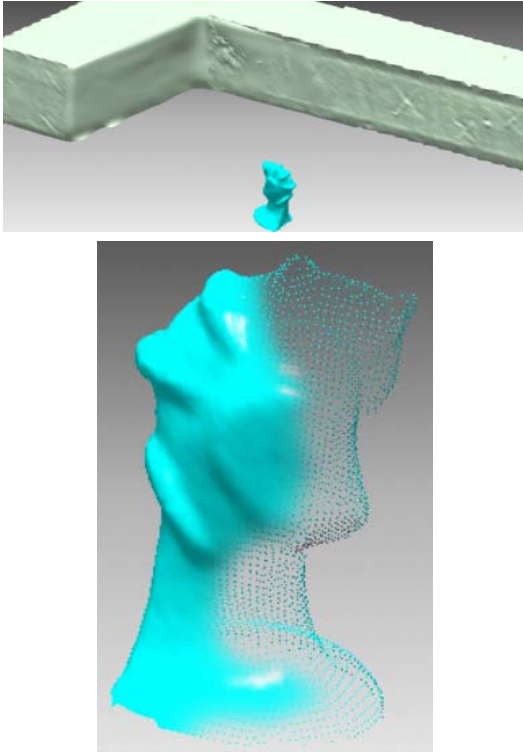
Figure 5. Top: 3D registration of the L-shaped object P and workpiece A_1. Bottom: Mesh and smoothed surface of A_1. The resolution of the scan is relatively poor.

Figure 6. 3D registration of P and workpiece A_2.

4. NUMERICAL RESULTS

We have applied the procedure of Fig. 4 to the two workpieces shown in Fig. 3. The digital representations ^{X}A of the workpieces A_1 and A_2 are shown in Figs. 5 and 6, respectively, together with the reference geometry ^{B}p. As mentioned, the shape of ^{X}A is relevant, whereas its local coordinate system X is arbitrary. ^{B}P needs to be determined only once, and then the set can be reused for several calibration processes, provided that the physical placement of P relative to B is not changed. The data sets ^{S}a and ^{S}p are taken from a constant scanning location. The two matching processes involve the minimization of $D(^{S}a, U(u)^{X}A)$ and of $D(^{S}p, V(v)\,^{B}P)$, or, alternatively, the minimization of the MDH distances. The final matrix W is computed using equation (1). If the scene is scanned from a different scanner location, the matrices U and V will in general be different from the matrices obtained previously. However, the matrix W is expected to be independent of the scanner's location.

First, we compared the results from one pair of sets ^{S}a and ^{S}p. The point cloud matching processes were repeated 10 times, and the principle axis rotation angles Ω of the resulting W matrices were determined. The histogram (Figure 7) shows a variation of Ω of approximately 1 degree, corresponding to about 0.4mm deviation near the surface of A_1.

For object A_1 we determined W and Ω from two different locations of the scanner (the scanner was displaced about half a meter, at approximately 1.2m scanning distance). Again, the difference between the Ω angles stayed well below 1 degree (Figure 8).
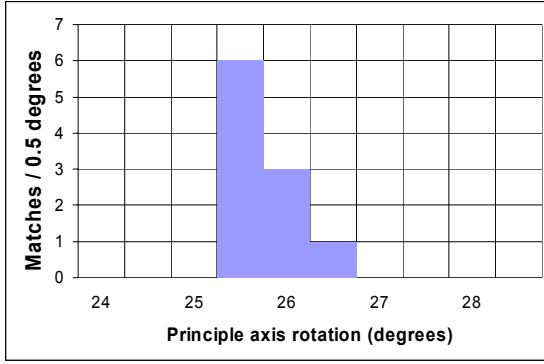
Figure 7. Matching accuracy for object A_1. Number of matches per interval of 0.5 degrees principle axis rotation Ω.
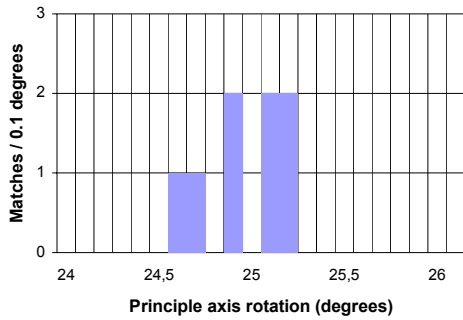

Figure 8. Ω distribution for object A_1. The matrix W was determined for two different locations of the scanner.
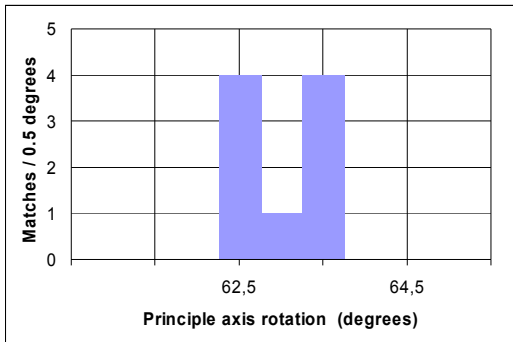

Figure 8. Ω distribution for object A_2. The matrix W was determined for five different locations of the scanner.

Workpiece A_2 was calibrated from five different scanning positions. In table 1, two out of five resulting matrices U, V and W are shown in terms of their Euler rotations and principle axis rotations. U and V differ significantly due to the change of position of the scanner. However, the W matrix is almost unchanged; their Ω difference is approximately 0.3 degrees.

The Ω-distribution from the five different calibration directions is presented in figure 9. The variation is about 1.5 degrees.

	φ(degr)	θ(degr)	ψ(degr)	Ω(degr)
$\underline{U}_1$	-144.48	32.82	134.41	34.29
$\underline{U}_2$	-168.18	44.28	155.37	46.00
$\underline{V}_1$	132.61	43.36	162.84	76.44
$\underline{V}_2$	131.59	57.89	152.26	92.92
$\underline{W}_1$	**110.25**	**48.93**	**-151.66**	**63.29**
$\underline{W}_2$	**109.20**	**47.61**	**-152.61**	**63.55**

Table 1. Euler angles and principle axis rotation for two different scanning positions for calibrating object A_2.

5. CONCLUSIONS AND FURTHER RESEARCH

The position of object frame X relative to a known reference frame B could be determined with precision sufficient for the Selective Clay Milling process (approximately 0.3 mm). If the object gets smaller than about 2cm, the width of the Ω distribution exceeds 1 degree, corresponding to about 0.2mm spatial deviation. A typical object, a manually crafted clay model for example, has a diameter 10 to 50cm or more. Objects with sizes in this range can be handled by our method.

The total time to obtain a calibration matrix, including scanning and running the software tool, is about 20 minutes.

A general problem is ambiguity due to object symmetry. If an object is (approximately) rotational symmetric, then it will be difficult to find the correct transformation.

Another assumption, thus far, is that the shape of the calibrated object is not significantly changed between the global scanning and the on-site scanning. Later, if needed, this assumption can be lifted by allowing, for example, local changes, or global changes that can be described using templates or deformation lattices.

When artificial features such as colored pins would be put onto the workpiece and onto the reference object, the calibration procedure might be improved. There are, however, disadvantages of these add-ons. First, the artificial features would have to be in place in *all* scans, that is both in the ^XA data and in the ^Sa data, which would be a practical burden. Further, artificial features might physically preclude particular set-ups of the

workpiece, they may damage it or partially obscure its surface. Therefore we continue to improve the method of feature-less calibration.

There are several opportunities to automate the procedure to a genuine self-calibration process. The main problem is that both the ICP method as the Hausdorff distance method, as numerically implemented, tend to a local minimum, dependent on the starting condition of the search. Without the introduction of artificial feature points, or operator intervention, it might be feasible to perform a general seek process in order to reach a global minimum. One could also think of features painted on the surfaces. In case the scanner can integrated color information with the 3D data, this could help to find the right transformation.

We have not yet applied the 7th degree of freedom (rotation table) of the Sculpturing Robot. However, when the workpiece is fixed onto the rotating table, then the calibration of the Sculpturing Robot system itself is sufficient to know the total transformation.

In the current implementation the various objects (workpiece, reference object) are selected by the user. Also the portions ^{S}a and ^{S}p are selected manually. Since the platform geometry, including the L-shaped object, can be regarded as a constant scene it is surely feasible to detect the workpiece automatically from the scanned data.

The accuracy could be enhanced using conventional CCD cameras. If the matrix W is determined with a reasonable accuracy, then the contours of all digital shapes are known relatively accurately. Suppose that the robot tool is directed towards the workpiece based on a matrix W. Then by using CCD vision of the workpiece and the robot tool, a final calibration matrix W' could be derived. As mentioned, instead of the Euler angle parameterization, quaternions can be used for more efficient searching. Work in this direction is currently in progress.

6. ACKNOWLEDGEMENTS

7. REFERENCES

[Besl 1992] Besl, P.J. and N.D. McKay, "A method for registration of 3-D shapes". IEEE Transactions on Pattern Analysis and Machine Intelligence, Vol. 14, No. 2, pp 239-255.

[Broek 1996] Broek, J.J. *et al*. Calibration of a Sculpturing Robot System. In:: Soy Yeng Chai (Eds.), Proc. 4th Int. Conf. on Control utomation, Robotics and Vision, Nayang Technical University, Singapore, 1996, pp 2152-2156

[González-Galván 2003] González-Galván, E.J. *et al*. An efficient multi-camera, multi-target scheme for the three-dimensional control of robots using uncalibratd vision. Robotics and Computer Integrated Manufacturing 19 (2003) 387-400.

[Craig 1989] Craig, J.J., Introduction to Robotics Mechanics and control. Addison-Wesley, Reading, 1989.

[Latombe 1991] Latombe, J-C, Robot Motion Planning. Kluwer Academic Publishers, Boston, 1991.

[Pessel 2003] Pessel, N. *et al*. Camera self-calibration in underwater environment. Proc. 11th Int. Conf. WSCG'2003, V. Skala (Ed.), Union Agency Science Press, Plzen, 2003, pp 104-110.

[Prieto 2003] Prieto, P.A. *et al*, A novel method for early formal developments using computer aided design and rapid prototyping technology. Journal of Engineering Manufacture, Vol. 217, Part B, pp 695-698.

[Spanjaard 2001] Spanjaard, S. *et al.*, "Comparing different fitting strategies for matching two 3D point sets using a multivariable minimizer" Proc. of the 2001 Computers and Information in Engineering Conference, DETC'01/CIE-21242, ASME, New York, 2001.

[Tangelder 1998] Tangelder, J.W.H *et al.*, "Interference-free NC machining using spatial planning and Minkowski operations". Journal of Computer-aided Design, Vol. 30, Nr. 4, 1998, pp 277-286.

[Váradi 1997] Váradi, T. *et al*. Reverse engineering of geometric models- an introduction. Computer-Aided Design, Vol. 29, Nr. 4, 1997, pp 255-268

[Veltkamp 2001] Veltkamp, R.C. Shape matching: similarity measures and algorithms. Proc. Shape Modeling International Conference, a. Pasko and M. Spagnuolo, Eds., Los Alamitos, IEEE, 2001, pp. 188-197.

.